

## Changes in the 300-mb North Circumpolar Vortex, 1963–2001

JAMES K. ANGELL

*NOAA/Air Resources Laboratory, Silver Spring, Maryland*

(Manuscript received 16 February 2005, in final form 19 October 2005)

### ABSTRACT

The mean monthly polar stereographic map analyses of the Free University of Berlin terminated at the end of 2001. This paper summarizes the changes in size of the 300-mb north circumpolar vortex, and quadrants, for the full period of record, 1963–2001, where the size has been defined by planimetry of the area poleward of contours in the jet stream core. A contracted vortex has tended to be a deep vortex in winter but a shallow vortex in summer. During 1963–2001 there was a statistically significant decrease in vortex size of 1.5% per decade, the decrease in size of Western Hemisphere quadrants being twice that of Eastern Hemisphere quadrants. A significant increase in Arctic Oscillation (AO) index accompanies the significant decrease in vortex size, but since the vortex contracts appreciably in all four seasons, whereas the positive trend in the AO index is mainly in winter, the vortex cannot serve as a proxy for the AO index. The evidence for vortex contraction at the time of the 1976–77 regime shift is not conclusive, but there is good evidence for a 6% increase in vortex size due to the 1991 Pinatubo eruption. There is little change in vortex size following the 1982 El Chichon eruption, however. Because on average there is a significant 4% contraction of the vortex following an El Niño, it is proposed that the vortex expansion to be expected following the 1982 El Chichon eruption has been contravened by the contraction following the strong 1982–83 El Niño. There is little relation between vortex size and phase of the quasi-biennial oscillation (QBO), and the evidence for a contracted vortex near 11-yr sunspot maxima is tenuous because the vortex record extends through only three full sunspot cycles. There is a highly significant tendency for opposite vortex quadrants 0°–90°E and 90°W–180° to vary in size together, indicating either a pulsating polar vortex or the propagation of planetary wavenumber 2.

### 1. Introduction

The Free University of Berlin Northern Hemisphere polar stereographic map series (Labitzke et al. 1986), prepared and analyzed by the Stratospheric Research Group of the Institute of Meteorology, was terminated at the end of 2001, partly because of the retirement of Karin Labitzke. This ended 39 yr of mean monthly analyses at the earth's surface, and at pressure surfaces of 700, 300, 100, 50, and 30 mb. These maps may be unparalleled in the care and dedication with which they were prepared and analyzed. This paper represents a final summary of the work I have carried out on the 300-mb north circumpolar vortex using these analyses, and includes discussion of the relation between 300-mb

vortex size, and vortex depth, midlatitude tropospheric temperature, and Arctic Oscillation (AO) and North Atlantic Oscillation (NAO) indexes.

A recent paper (Frauenfeld and Davis 2003), based on the Ph.D. dissertation of the former, goes into great detail on the variation in the north circumpolar vortex between 1949 and 2000, as estimated from National Centers for Environmental Prediction–National Center for Atmospheric Research (NCEP–NCAR) reanalysis (Kalnay et al. 1996; Kistler et al. 2001). Frauenfeld and Davis define the north polar vortex for each month by means of the geopotential height contour that most consistently is in the core of the jet stream westerlies at 700, 500, and 300 mb. The latitudes at which these contours intersect the 72 meridians at 5° longitude intervals are then averaged to provide the mean monthly latitudes for the vortex. Contours farther to the north and south are similarly treated at each of the three pressure surfaces. These data have been standardized with respect to each month's mean to provide a "standardized latitude." I, on the other hand, measure by planimeter

---

*Corresponding author address:* Dr. James K. Angell, NOAA/Air Resources Laboratory, 1315 East–West Highway, Silver Spring, MD 20910.  
E-mail: marcia.wood@noaa.gov

(an instrument for measuring the area of a plane figure by tracing the perimeter of the figure) the monthly size of the 300-mb north circumpolar vortex, and its quadrants, poleward of a seasonally varying contour chosen also to be in the core of the jet stream westerlies.

Frauenfeld and Davis (2003) have provided an excellent summary of previous work dealing with the north polar vortex as well as a fine literature review, which is not repeated here.

## 2. Procedures

The mean monthly analyses of the Institute of Meteorology of the Free University of Berlin are on Northern Hemisphere polar stereographic maps, or map projections centered on the North Pole. The analyses are hand produced, using such tools as thermal wind to ensure continuity between pressure surfaces. The 300-mb height surface is used in this and previous analyses (Angell and Korshover 1975, 1977, 1978, 1985; Angell 1992, 1998, 2001) because the north circumpolar vortex is best defined at this jet stream level near the top of the troposphere. The 300-mb geopotential height contours chosen to delimit the vortex are the ones in the core of the jet stream, namely, in winter [December–February (DJF; hereafter, 3-month periods are denoted by the first letter of each respective month)] the 9120-m contour at about 40°N, in spring (MAM) the 9280-m contour also at about 40°N, in summer (JJA) the 9440-m contour at about 50°N, and in fall (SON) the 9280-m contour at about 45°N. Thus, the vortex defined here comprises 20%–30% of the hemisphere area. For comparison, the “center” 300-mb mean monthly contours chosen by Frauenfeld and Davis (2003) are the 9120-m contour in winter, the 9120- and 9240-m contours in spring, the 9360-m contour in summer, and the 9360-, 9240-, and 9120-m contours in fall.

Figure 1 shows examples of the height contours on polar stereographic maps, where NP is the North Pole. The size of the 300-mb north polar vortex, and its quadrants, is estimated by planimetry of the area poleward of these contours. Repeated planimetry shows that the uncertainty in the measurement of vortex size on the mean monthly Berlin, Germany, maps is about 1% so that, dividing by the square root of number of months, the uncertainty in seasonal vortex size is about 0.6% and annual vortex size is about 0.3%. The uncertainty in quadrant size is, of course, 4 times as great. In the following, “vortex” always refers to the 300-mb north circumpolar vortex, and the period of record is always 1963–2001. In the figures, vortex and quadrant sizes are anomalies in percent, temperatures are anomalies in kelvins, and north polar 300-mb heights

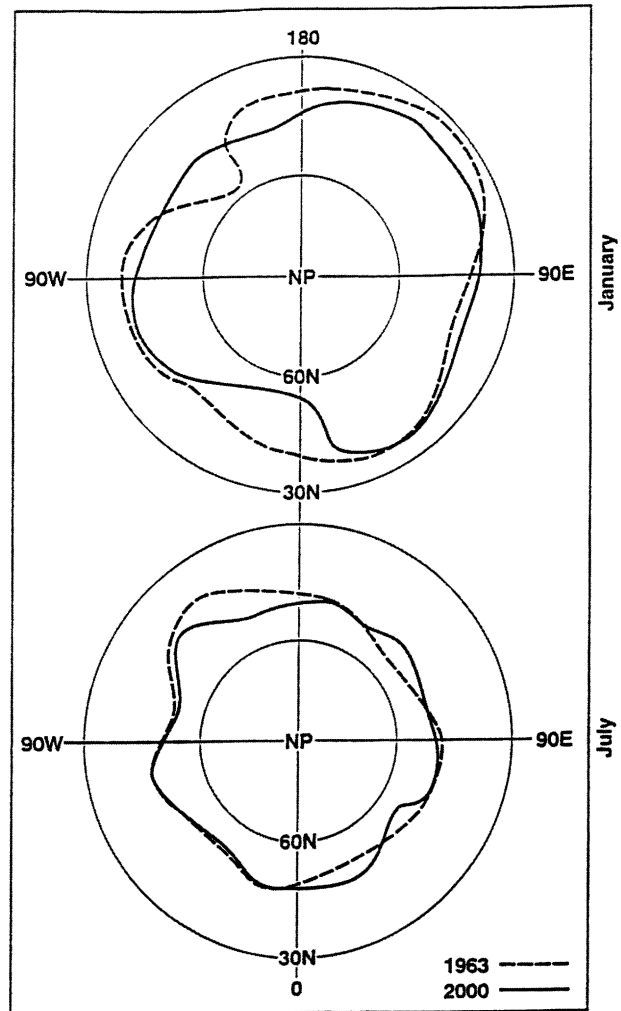


FIG. 1. Based on Free University of Berlin mean monthly polar stereographic maps centered on the North Pole (NP): (top) the 300-mb height contour of 9120 m in January of 1963 (dashed line) and 2000 (solid line), and (bottom) the 9440-m height contour in July of these years. The size of the vortex and its quadrants is estimated by planimetry of the area poleward of these contours (and the 9280-m contour in spring and fall) in the core of the jet stream.

are anomalies in meters, where all anomalies are computed as deviations from the seasonal mean for the period 1963–2001.

## 3. Comparison of vortex size with vortex depth and tropospheric temperature

The middle trace of Fig. 2 shows the variation in annual size of the vortex, expressed as a percentage deviation from the mean size for the 1963–2001 period of record. Based on linear least squares regression (the

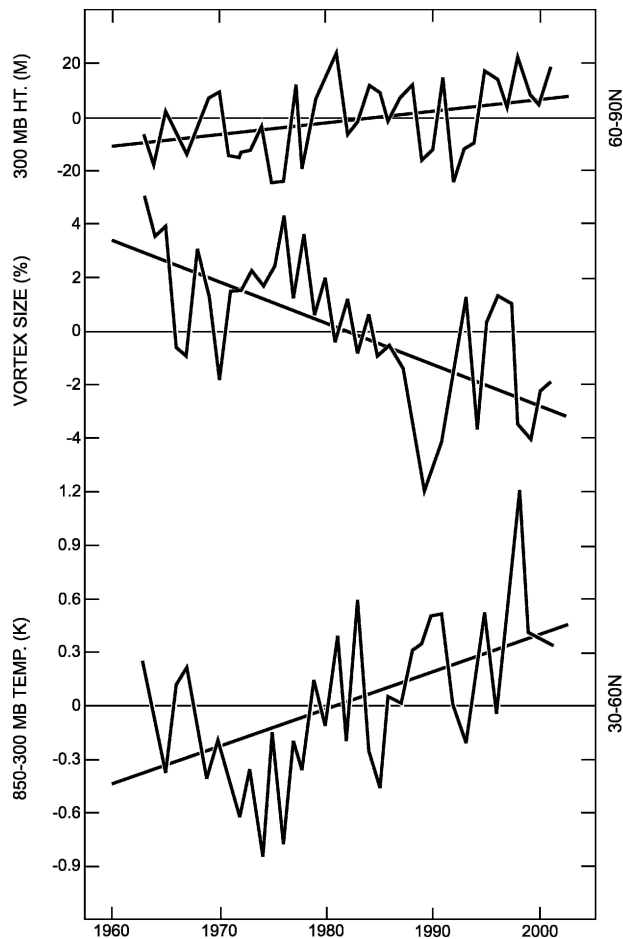


FIG. 2. Variation in (middle) annual 300-mb vortex size anomaly in percent, (bottom) north temperate 850–300-mb temperature anomaly in kelvins and (top) north polar 300-mb height anomaly in meters, the latter of which is an inverse measure of vortex depth. Straight lines are linear regression lines, and vortex size and temperature ordinates are compatible based on the hydrostatic equation.

straight lines in Fig. 2), the trend in annual vortex size is  $-1.5 \pm 1.4\%$  decade $^{-1}$  (see Table 1), where the 95% confidence interval is 2 standard errors of estimate of the linear regression. Thus, the decrease in vortex size during this period is statistically significant. In Table 1, the larger percentage decrease in vortex size in summer would be expected because of the smaller size of the vortex in that season (see Fig. 1).

The trace at top in Fig. 2 shows the variation in annual average height of the 300-mb surface in the north polar zone ( $60^{\circ}$ – $90^{\circ}$ N), based on NCEP–NCAR reanalysis (Kalnay et al. 1996; Kistler et al. 2001). The increase in annual height of  $4.3$  m decade $^{-1}$  (decrease in vortex depth) is not quite significant (see Table 1), hardly surprising since the trend in winter is opposite to the trend in the other three seasons. The correlations at right in Table 1 show that in winter a contracted vortex tends to be a deep vortex, similar to the finding of Holton and Tan (1980) for the stratospheric 50-mb surface, whereas in summer a contracted vortex tends to be a shallow vortex. This presumably reflects the tendency for the vortex to be a dynamic entity in winter but a thermal entity in summer. These differing senses of winter and summer correlation are significant at 1% and 5% levels, respectively.

The trace at bottom in Fig. 2 shows the variation in annual 850–300-mb temperature (expressed as a deviation from the mean temperature in kelvins) in the north temperate zone ( $30^{\circ}$ – $60^{\circ}$ N), as estimated from 12 radiosonde stations in this zone (Angell 2003). Table 1 shows that the trend in annual temperature for the period 1963–2001 is  $0.20 \pm 0.18$  K decade $^{-1}$ . Thus, just as the tendency for contraction of the vortex is barely significant, so is the tendency for warming of the north temperate zone during this period.

TABLE 1. At left are the trends for 1963–2001 in seasonal and annual 300-mb vortex size, 850–300-mb temperature in the north temperate zone ( $30^{\circ}$ – $60^{\circ}$ N), and average height of the 300-mb surface in the north polar zone ( $60^{\circ}$ – $90^{\circ}$ N), the latter an inverse measure of vortex depth. The appended 95% confidence intervals are two standard errors of estimate of the linear regression. At right is the correlation between vortex size, and this temperature and height, the significance taking into account serial correlation and indicated by sigma ( $\sigma$ ), where  $2\sigma$  is the 5% significance level, etc.

	Trend			Correlation			
	Vortex size (% decade $^{-1}$ )	850–300-mb temperature (K decade $^{-1}$ )	300-mb height (m decade $^{-1}$ )	Vortex temperature		Vortex height	
				Correlation	Significance ( $\sigma$ )	Correlation	Significance ( $\sigma$ )
DJF	$-1.3 \pm 1.6$	$0.23 \pm 0.21$	$-5.7 \pm 11.6$	–0.41	2.2	0.56	3.3
MAM	$-0.8 \pm 1.0$	$0.22 \pm 0.15$	$9.2 \pm 6.5$	–0.42	2.7	–0.09	0.5
JJA	$-2.7 \pm 2.2$	$0.30 \pm 0.14$	$6.5 \pm 4.3$	–0.87	6.6	–0.41	2.6
SON	$-1.4 \pm 1.3$	$0.10 \pm 0.15$	$6.4 \pm 7.5$	–0.55	3.7	–0.02	0.1
Year	$-1.5 \pm 1.4$	$0.20 \pm 0.18$	$4.3 \pm 4.6$	–0.67	3.4	–0.24	1.2

The compatibility of the  $1.5\%$  decade<sup>-1</sup> vortex contraction, and  $0.20\text{ K decade}^{-1}$  midlatitude tropospheric warming, may be estimated from the hydrostatic equation and the geostrophic wind equation. The former shows that a surface–300-mb temperature increase of  $0.20\text{ K decade}^{-1}$  leads to about a  $7\text{ m decade}^{-1}$  increase in 300-mb height. Accepting the value of  $20\text{ m s}^{-1}$  for the mean annual zonal geostrophic wind at 300 mb (Rosen and Gutowski 1992), the contour spacing associated with that wind means that the 300-mb contours must move poleward at the rate of  $0.31^\circ$  latitude decade<sup>-1</sup> in order to realize the height change of  $7\text{ m decade}^{-1}$ . At the latitude of  $45^\circ\text{ N}$ , this is a percentage change in latitude of  $0.7\%$  decade<sup>-1</sup>, which, from the relation between radius and area of a circle, translates to a change of  $1.5\%$  decade<sup>-1</sup> in vortex size, the value actually observed. While this exact agreement is, of course, fortuitous, it does suggest that the indicated decrease in size of the vortex during 1963–2001 is basically in accord with the indicated increase in 850–300-mb temperature in the north temperate zone as estimated from the 54-station radiosonde network.

Frauenfeld and Davis (2003) find, based on NCEP–NCAR reanalysis, an increase in the standardized latitude of their “center contour” of  $0.13^\circ$  latitude decade<sup>-1</sup> for the period 1970–2000 (see their Fig. 2 at top and Table 2 at top), compared to the value of  $0.31^\circ$  latitude decade<sup>-1</sup> for the period 1963–2001 obtained from the Berlin maps. Despite the difference in data and analysis procedure, and in my case the approximations involved in passing from vortex size to contour latitude, I find this factor-of-2 difference disturbingly large, but at least there is agreement that there has been an appreciable contraction of the vortex during the last three decades.

Table 1 shows that the correlation between 300-mb vortex size and 850–300-mb temperature is significant in all seasons, with the correlation of  $-0.87$  in summer significant at the 6 sigma level, and the annual correlation of  $-0.67$  significant at the 3 sigma level. Thus, the seasonal and annual variations in 300-mb vortex size, and midlatitude 850–300-mb temperature, are closely related, as they should be.

#### 4. Comparison of vortex and quadrant size with NAO and AO indexes

It is useful to compare the variation in the size of the vortex with the variation in the NAO index and AO index to see to what extent the vortex provides similar information and to what extent it does not. The familiar NAO index of NCEP (Barnston and Livezey 1987) is chosen here. Basically, this index measures the mean

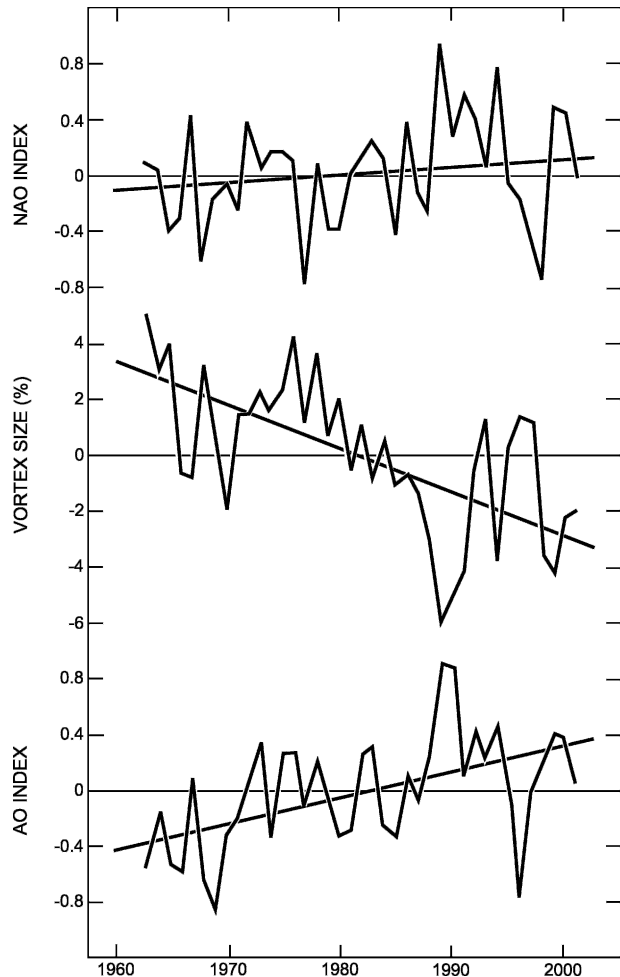


FIG. 3. Comparison of the variation in (middle) annual 300-mb vortex size with normalized values of (bottom) an AO index and (top) NAO index.

monthly difference in 700-mb height between Azores and Greenland. For the AO index, the one proposed by Li and Wang (2003) is used, which is simply the difference in surface pressure between  $35^\circ$  and  $65^\circ\text{ N}$  around the hemisphere based on NCEP–NCAR monthly reanalysis data. In their paper, Li and Wang (2003) find that this simple AO index has a more symmetric correlation with surface pressure anomalies around the hemisphere than does the leading empirical orthogonal function of Thompson and Wallace (1998) and Wallace (2000).

Figure 3 compares the variation in annual size of the vortex (middle) with the variation in annual NAO index defined by NCEP (top) and the variation in annual AO index defined by Li and Wang (2003), the latter two in normalized units. The inverse relation between vortex size and AO is more impressive than that be-

TABLE 2. Same as in Table 1, except comparison of seasonal and annual vortex size with normalized AO and NAO indexes.

	Trend			Correlation			
	Vortex size (% decade <sup>-1</sup> )	AO index (decade <sup>-1</sup> )	NAO index (decade <sup>-1</sup> )	Vortex-AO		Vortex-NAO	
				Correlation	Significance ( $\sigma$ )	Correlation	Significance ( $\sigma$ )
DJF	-1.3 ± 1.6	0.59 ± 0.56	0.32 ± 0.27	-0.82	4.6	-0.72	4.1
MAM	-0.8 ± 1.0	0.04 ± 0.19	0.10 ± 0.18	-0.53	3.1	-0.36	2.1
JJA	-2.7 ± 2.2	0.05 ± 0.08	-0.10 ± 0.19	-0.49	3.1	0.03	0.2
SON	-1.4 ± 1.3	0.03 ± 0.13	-0.04 ± 0.19	-0.37	2.3	0.06	0.3
Year	-1.5 ± 1.4	0.18 ± 0.18	0.05 ± 0.10	-0.58	2.8	-0.34	2.1

tween vortex size and NAO, to be expected because both 300-mb vortex size and AO index reflect hemispheric changes. Thus, Table 2 shows that the (negative) correlations between vortex size and AO index are always greater in magnitude than those between vortex size and NAO index, and the former are always significant at the 5% level whereas the latter are not. A striking difference between vortex size and AO index, however, is that the vortex has contracted appreciably in all four seasons of the year, whereas the positive trend in annual AO index results almost entirely from the trend in winter. Thus, vortex size cannot serve as a proxy for the AO or the NAO index.

Table 3 presents the correlations, and their significance, between the size of the vortex quadrants and AO and NAO indexes. All quadrant sizes except for 0°–90°E are significantly (at the 5% level) correlated with the AO index. However, the NAO index is only significantly correlated with the size of quadrant 0°–90°W, the latter significance to be expected because both Greenland and Azores are within this quadrant. Note that quadrant 0°–90°W also has the highest and most significant correlation with the AO index, adding to the evidence that the NAO and AO indexes are “two paradigms, one phenomenon” (Wallace 2000).

### 5. Relation of vortex size to the 1976–77 regime shift

Trenberth (1990) was the first to define the large warming signal in global temperature in 1976–77 as a

TABLE 3. Correlation between the annual sizes of the vortex and its quadrants, and AO and NAO indexes, for the period 1963–2001. Significance is as in Table 1.

	AO		NAO	
	Correlation	Significance ( $\sigma$ )	Correlation	Significance ( $\sigma$ )
0°–90°E	-0.14	0.8	0.03	0.2
90°E–180°	-0.46	2.3	-0.13	1.5
90°W–180°	-0.47	2.0	-0.30	1.8
0°–90°W	-0.66	4.0	-0.61	4.2
Vortex	-0.58	2.8	-0.34	2.1

regime or climate shift, with follow-up discussions by Trenberth and Hurrell (1994) and Hurrell (1996) among others. As an example, based on a 54-station global radiosonde network (Angell 2003), there is a global 850–300-mb warming of 0.6 K, between 1976 and 1977, and tropical (30°S–30°N) 850–300-mb warming of 0.8 K between these two years. This warming has also been referred to as a Pacific climate shift (Miller et al. 1994).

The vertical dotted line in Fig. 4 defines the time of the 1976–77 regime shift in relation to Singapore 50-mb zonal wind [quasi-biennial oscillation (QBO)], 300-mb vortex size (trace second from the top), Niño-3 SST, and sunspot number, where all traces have been smoothed by a binomial weighting of successive seasonal anomalies expressed as deviations from their seasonal means. There is an abrupt 5% decrease in vortex size just at the time of the regime shift, from the maximum size for the period of record to the average size for that period. The problem with considering this abrupt change as a regime shift is the 3% increase in vortex size only a year earlier, so that the trace looks more like a peak than a regime shift. It is surprising that a major event such as a regime shift does not show up unambiguously in a basic circulation feature such as the 300-mb north circumpolar vortex.

### 6. Impact of Pinatubo and El Chichon eruptions on vortex size

The vortex trace in Fig. 4 shows about a 5% increase in vortex size immediately following the Pinatubo eruption in the summer of 1991. Based on the 54-station network, the binomially smoothed north temperate 850–300-mb temperature decreased by about 0.8 K at this time, compatible with this increase in vortex size. Because it is generally accepted that the Pinatubo eruption did indeed cause a cooling of the troposphere, even on a global scale (e.g., Free and Angell 2002; Fig. 6), there seems to be no reason to doubt that the increase in vortex size following this eruption is due to the eruption.

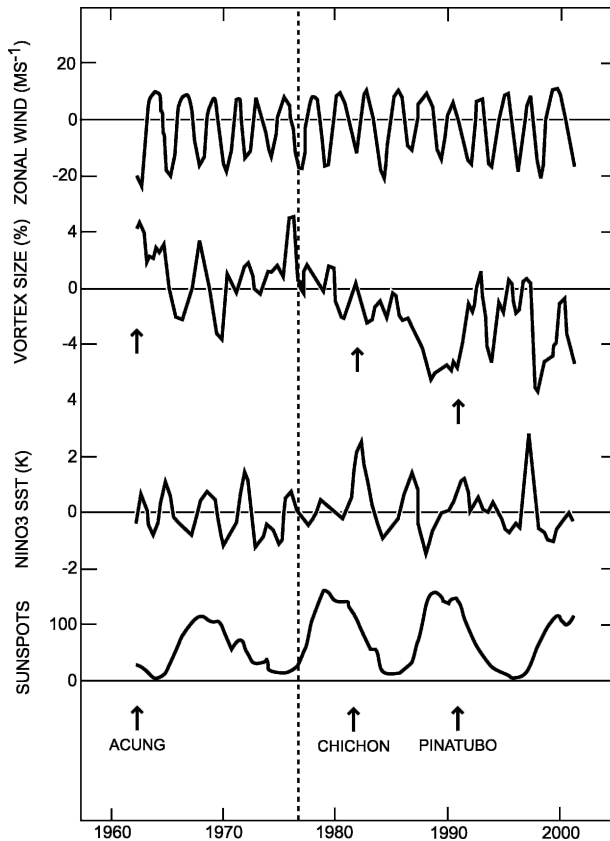


FIG. 4. Comparison, from top to bottom, of 50-mb zonal wind at Singapore (QBO), vortex size, Niño-3 SST, and sunspot number, where a binomial weighting has been applied to successive seasonal anomalies from seasonal averages. The times of major volcanic eruptions are indicated by vertical arrows, and the 1976–77 regime shift is indicated by the vertical dotted line.

Figure 4 also shows, however, that there was no appreciable change in vortex size following the El Chichon eruption in the spring of 1982. Though the El Chichon eruption was weaker, and the volcanic ash not as globally distributed as following the Pinatubo eruption, this cannot explain the dramatic difference in vortex size change following the two eruptions. I propose that the main reason for this difference is the strong El Niño of 1982–83 (see the trace third from the top in Fig. 4) and the contravening effect the vortex contraction tending to follow such an El Niño (see the middle diagram of Fig. 5) would have on the vortex expansion induced by the El Chichon eruption. I am not claiming that the two effects are additive in a simple linear way, just that they are influencing each other.

The timing is about right for such a cancellation effect. The smoothed Niño-3 SST maximum follows the El Chichon eruption by three seasons, and Fig. 5 indicates that the maximum in vortex size tends to occur about four seasons after the Niño-3 SST maximum.

Therefore, if the time between the El Chichon eruption and the maximum vortex size resulting from the eruption were seven seasons, there would tend to be a cancellation of El Niño and volcanic influences. The time between Pinatubo eruption and smoothed maximum vortex size was 8 seasons, so if the two eruptions are similar in the timing of their effects, the proposed near cancellation of El Niño and volcanic effects following El Chichon appears reasonable. Unfortunately, because the Agung eruption occurred only one season after the beginning of the vortex record, its volcanic impact cannot be defined, so it is of no help in resolving this issue.

### 7. Impact of QBO, El Niño, and sunspot number on vortex size

As in the previous vortex paper (Angell 2001), the superposed epoch method (Panofsky and Brier 1958) is used to quantify the impact on vortex size of the QBO (50-mb zonal wind at Singapore), Niño-3 SST (average sea surface temperature from 5°S to 5°N between 90°W and 150°W), and sunspot number, the variations of which are shown in Fig. 4. Besides the addition of another year of vortex data, changes from the previous study include the filling in of several missing monthly maps by mailings from the Free University of Berlin, the use of monthly rather than seasonal data to estimate the impact of QBO on vortex size, and extension of the study of the impact of El Niño on vortex size from six seasons to eight seasons before and after SST maximum. Because of the considerable impact of the Pinatubo eruption on vortex size, to avoid contamination of the superimposed epoch analysis the QBO and El Niño cycles bracketing the Pinatubo eruption are not considered, and years 1992 and 1993 are excluded from the sunspot number analysis.

Figure 5 shows the vortex size as a function of number of months from QBO 50-mb east wind maximum at Singapore (left), number of seasons from Niño-3 SST maximum (middle), and number of years from sunspot number maximum (right). The difference in time scales should preclude much interference among relations. There is little evidence of a relation between phase of the QBO and 300-mb vortex size in this dataset (only a slight tendency for vortex contraction about two months before QBO east wind maximum) even though an earlier paper (Angell 1992) found, based on the 300-mb vortex data through 1989, the vortex to be 1.5% smaller in the west wind phase of the QBO than in the east wind phase. The latter is in agreement with the finding of Holton and Tan (1980) for a contracted 50-mb (stratospheric) vortex in the west wind phase of the

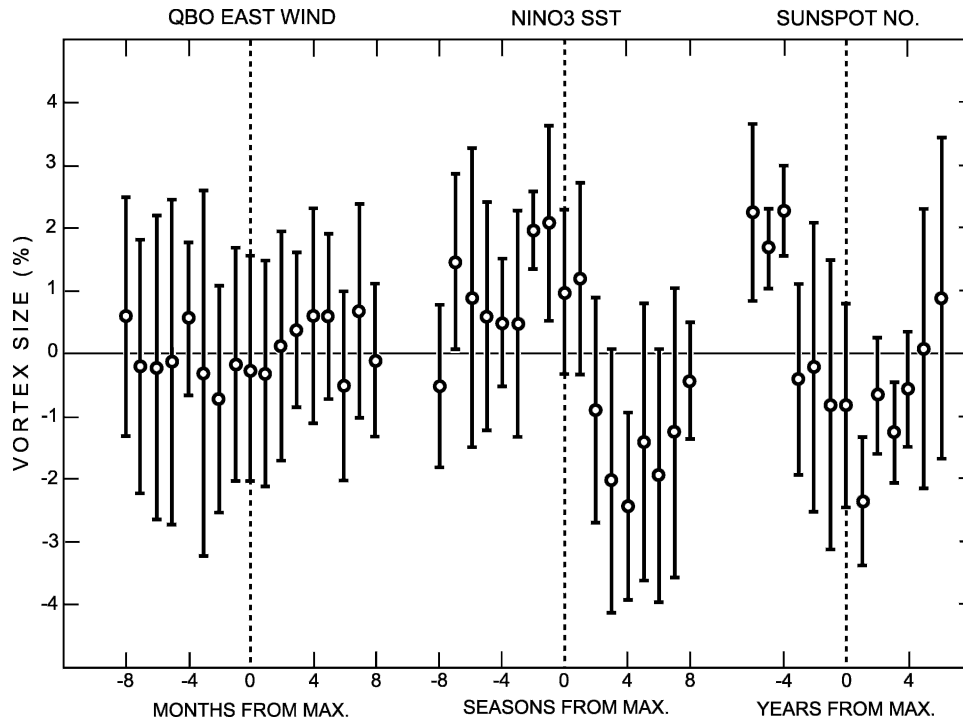


FIG. 5. Based on the superposed epoch method, vortex size from (left) eight months before to eight months after QBO (Singapore 50 mb) east wind maximum, (middle) eight seasons before to eight seasons after Niño-3 SST maximum, and (right) six years before to six years after sunspot number maximum. Vertical bars extend  $\pm 2$  standard deviations of the mean based on 17, 8, and 3 cases, respectively.

QBO. The change in result with the addition of only 12 yr of data shows how fragile some of these relations are.

Much more impressive is the significant tendency (nonoverlapping vertical bars) for the vortex to be most expanded one–two seasons before Niño-3 SST maximum, and most contracted about 1 yr after this maximum. Figure 6 shows that it is quadrant  $90^{\circ}\text{W}$ – $180^{\circ}$  (El Niño quadrant) that has the most significant tendency to be expanded near SST maximum, a finding also of Frauenfeld and Davis (2000, 2002), and contracted thereafter. Opposite quadrant  $0^{\circ}$ – $90^{\circ}\text{E}$  also shows a good tendency for contraction following the Niño-3 SST maximum.

The right-hand diagram in Fig. 5 indicates a tendency for contraction of the vortex near sunspot maxima, but the annual sizes are erratic, not surprising since there are only three full 11-yr solar cycles available. Figure 7 shows vortex size as a function of sunspot number, but differentiated according to whether the vortex size is in the east or west wind phase of the QBO (top trace in Fig. 4). In agreement with the findings of Labitzke (1987) and van Loon and Labitzke (1988), there is more of a tendency for vortex contraction with increase in sunspot number in the west wind than east wind phase

of the QBO with, in the west wind case, significant differences in vortex size (nonoverlapping horizontal bars) for sunspot numbers less than 50 in comparison with sunspot numbers between 100 and 150. An informative summary of this and other findings related to the possible connection between stratospheric circulation and sunspot number can be found in a recently published book by Labitzke and van Loon (1999).

## 8. Changes in quadrant size, and the correlations among the sizes

Table 4 shows at left the trends in annual size of the vortex quadrants. While all quadrants decreased in size, the trends vary by a factor of 4. Note that the decrease in size of Western Hemisphere quadrants averages twice that of Eastern Hemisphere quadrants.

Figure 8 shows the variation in the percent of the vortex in each quadrant. There is symmetry in the trends, quadrants  $0^{\circ}$ – $90^{\circ}\text{E}$  and  $90^{\circ}\text{E}$ – $180^{\circ}$  showing relatively small and large increases in percent of vortex, and quadrants  $90^{\circ}\text{W}$ – $180^{\circ}$  and  $0^{\circ}$ – $90^{\circ}\text{W}$  showing relatively large and small decreases in percent of vortex. Table 4 quantifies the results of Fig. 8 by presenting at right the

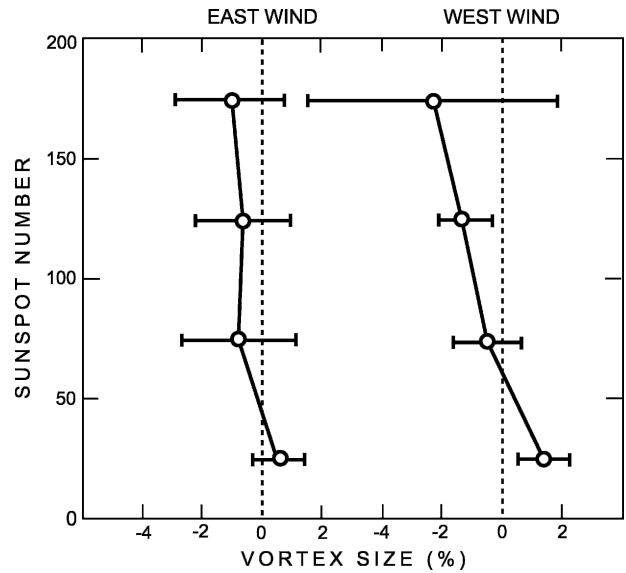
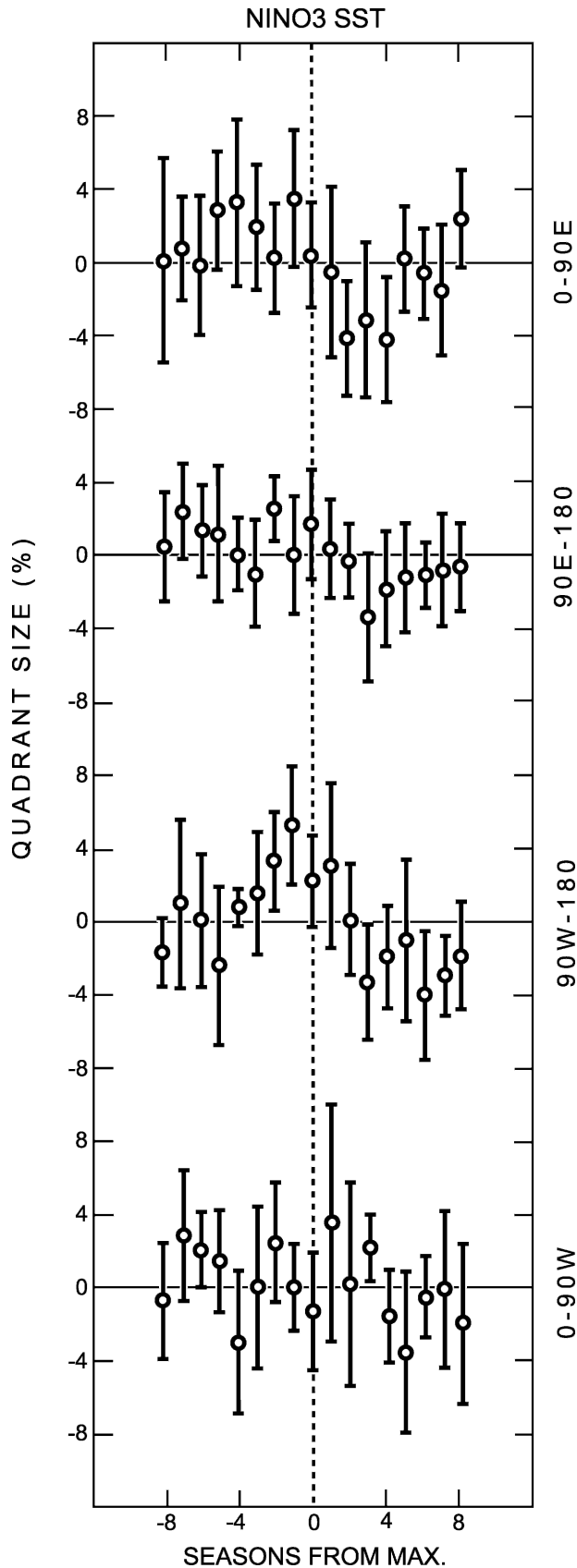


FIG. 7. Variation of vortex size with sunspot number during (left) east wind and (right) west wind phases of the QBO, as estimated from 156 seasonal values (nearly half for sunspot number less than 50). Horizontal bars extend two standard deviations of the mean on both sides of the mean.

average percent of the vortex in each quadrant, as well as the change in this percent during 1963–2001. Quadrant 90°E–180° is the largest quadrant being almost 27% of the vortex, and it is also the quadrant showing the largest increase in percent of vortex, a significant 0.23% decade<sup>-1</sup>. While it is not the smallest quadrant, the adjacent El Niño quadrant, 90°W–180°, shows the compensating (and significant) decrease in percent of vortex of 0.22% decade<sup>-1</sup>. These significant trends of opposite sense in the Pacific Ocean area imply circulation changes there.

Summing the percent of the vortex in opposite quadrants provides an estimate of vortex ellipticity. The middle column of Table 4 shows that, on average during 1963–2001, quadrants 90°E–180° and 0°–90°W made up 50.2% of the vortex so that, based on the quadrants used here, the 300-mb north circumpolar vortex is nearly circular. Such near circularity might not be found if the quadrants were based on vortex position and shape, as suggested by a reviewer. The ellipticity of polar stratospheric vortices has been examined by Waugh (1997).

←

FIG. 6. Based on the superposed epoch method, the size of each (top to bottom) vortex quadrant from eight seasons before to eight seasons after the Niño-3 SST maximum. Vertical bars extend ±2 standard deviations of the mean based on eight cases.

TABLE 4. At left is the trend in annual size of the vortex and its quadrants for the period 1963–2001, with confidence intervals as in Fig. 1. At right is the average percent of the vortex in each quadrant during this period, and its trend and confidence interval.

	Trend (% decade <sup>-1</sup> )	Percent of vortex	
		Avg (%)	Trend (% decade <sup>-1</sup> )
0°–90°E	-1.3 ± 1.6	25.1	0.06 ± 0.18
90°E–180°	-0.6 ± 0.8	26.9	0.23 ± 0.18
90°W–180°	-2.3 ± 1.8	24.7	-0.22 ± 0.17
0°–90°W	-1.7 ± 1.5	23.3	-0.08 ± 0.20
Vortex	-1.5 ± 1.4		

Table 5 presents the correlations between detrended annual values of quadrant size (left), and between seasonal values of quadrant size determined as the deviation from binomially smoothed annual values (right), for opposite (top) and adjacent quadrants. The most striking feature is the positive correlation, significant at

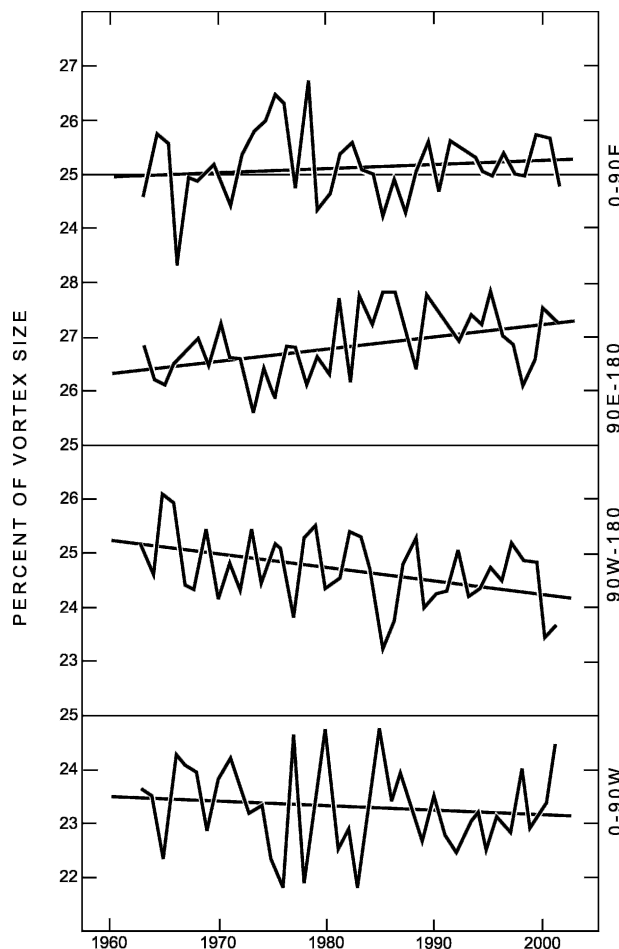


FIG. 8. Variation in the percent of the annual vortex size in each of the (top to bottom) vortex quadrants.

the 1% level, between the size of opposite quadrants 0°–90°E and 90°W–180°. These two quadrants tend to vary in size together, suggesting a pulsation of the vortex with the major axis alternating between 90°E–180°, 0°–90°W and 90°W–180°, 0°–90°E or, as suggested by a reviewer, simply the propagation of planetary wave-number 2. Seasonally, there is also a significant negative correlation between the size of adjacent quadrants 0°–90°E and 0°–90°W, reflecting the well-known “see-saw” in surface pressure, and other quantities, between Europe and the western Atlantic (van Loon and Rogers 1978).

## 9. Summary

Following are the main findings from this study of the 300-mb north circumpolar vortex, based on 39 yr (1963–2001) of mean monthly polar stereographic maps prepared and analyzed by the Stratospheric Research Group of the Institute of Meteorology of the Free University of Berlin.

- 1) A contracted vortex tends to be a deep vortex in winter but a shallow vortex in summer
- 2) There is a statistically significant decrease in annual vortex size of 1.5% decade<sup>-1</sup>, compatible with the significant increase in annual north temperate 850–300-mb temperature of 0.20 K decade<sup>-1</sup>.
- 3) The significant decrease in annual vortex size is associated with a significant increase in an Arctic Oscillation (AO) index, but since the vortex has contracted appreciably in all four seasons whereas the positive trend in AO index is mainly in winter, the vortex cannot serve as a proxy for the AO index.
- 4) There is a 5% decrease in vortex size at the time of the 1976–77 regime shift, but the extent to which this actually reflects the shift is uncertain because of a 3% increase in vortex size a year earlier.
- 5) There is a 6% increase in vortex size following the 1991 Pinnatubo eruption, but little change in vortex size following the 1982 El Chichon eruption; the latter proposed to result from the contravening effect of the vortex contraction induced by the strong 1982–83 El Niño.
- 6) The significant tendency for the vortex to be about 4% larger one–two seasons before the Niño-3 SST maximum than four seasons after this maximum is best expressed in the El Niño quadrant 90°W–180°.
- 7) The tendency for the vortex to be contracted near sunspot maxima, that is, for a decrease in vortex size with increase in sunspot number, is more obvious in the west wind than east wind phase of the QBO.

TABLE 5. Correlation between the size of (top) opposite vortex quadrants and (bottom) adjacent vortex quadrants, based on (left) detrended annual quadrant size anomalies and (right) the deviation of seasonal quadrant size anomalies from binomially smoothed annual anomalies. Significance is as in Table 1.

Quadrants	Annual		Seasonal	
	Correlation	Significance ( $\sigma$ )	Correlation	Significance ( $\sigma$ )
0°–90°E, 90°W–180°	0.53	3.3	0.34	4.4
90°E–180°, 0°–90°W	0.24	1.3	–0.04	0.5
0°–90°E, 90°E–180°	0.33	1.9	0.11	1.4
90°E–180°, 90°W–180°	0.24	1.3	0.17	2.1
90°W–180°, 0°–90°W	–0.13	0.8	–0.15	1.9
0°–90°W, 0°–90°E	–0.12	0.7	–0.22	2.8

- 8) All vortex quadrants decreased in size during 1963–2001, but the decrease in size of Western Hemisphere quadrants averaged twice that of Eastern Hemisphere quadrants.
- 9) Quadrant 90°E–180° is the largest quadrant and shows the largest increase in percent of the vortex during 1963–2001. Quadrant 0°–90°W is the smallest quadrant, but it is El Niño quadrant 90°W–180° that shows the largest decrease in percent of the vortex during this period.
- 10) The tendency for the size of opposite vortex quadrants 0°–90°E and 90°W–180° to be large or small in the same season or year is significant at the 0.1% level, suggesting either a pulsating vortex or the propagation of planetary wavenumber 2.

With the termination of the Berlin map series, I terminate my own work in this “vortex” field. Despite the early recognition of the north circumpolar vortex as a basic circulation feature of the Northern Hemisphere (e.g., Willett 1949), the size of the 300-mb north polar vortex per se has not caught on as a useful tool in the study of global warming, even though the size represents an integration of tropospheric temperature around the hemisphere in midlatitudes good to about 0.1 K on mean monthly maps and is an easy concept to visualize and grasp. If the vortex position could be reliably estimated (which it could not in this analysis because of the imprecise measurement of quadrant size), the vortex might be considered a Lagrangian entity allowing for estimates of the changes at fixed points (such as the NAO index) due to movement of the vortex (vortex position) and change following the vortex (vortex size).

*Acknowledgments.* Karin Labitzke and the staff of the Institute of Meteorology of the Free University of Berlin have been most generous in providing me with polar stereographic maps in near-real time. Barbara Naujokat furnished me with the maps to fill in data gaps. Julian Wang of the NOAA per Air Resources

Laboratory (ARL) provided the data for AO and NAO indexes and also calculated the height of the 300-mb surface in the north polar zone from reanalysis data. I thank Bruce Eder, Melissa Free, and Dian Seidel of ARL for reviewing the initial manuscript, and four anonymous reviewers for unusually thorough and useful comments that resulted in considerable alteration, as well as some condensation, of the paper.

#### REFERENCES

- Angell, J. K., 1992: Relation between 300-mb north polar vortex and equatorial SST, QBO, and sunspot number and the record contraction of the vortex in 1988–89. *J. Climate*, **5**, 22–29.
- , 1998: Contraction of the 300 mbar north circumpolar vortex during 1963–1997 and its movement into the eastern hemisphere. *J. Geophys. Res.*, **103**, 25 887–25 894.
- , 2001: Relation of size and displacement of the 300 mbar north circumpolar vortex to QBO, El Niño, and sunspot number, 1963–2001. *J. Geophys. Res.*, **106**, 31 787–31 794.
- , 2003: Effect of exclusion of anomalous tropical stations on temperature trends from a 63-station radiosonde network, and comparison with other analyses. *J. Climate*, **16**, 2288–2295.
- , and J. Korshover, 1975: Evidence for a quasi-biennial variation in eccentricity of the north polar vortex. *J. Atmos. Sci.*, **32**, 634–635.
- , and —, 1977: Variation in size and location of the 300 mb north circumpolar vortex between 1963 and 1975. *Mon. Wea. Rev.*, **105**, 19–25.
- , and —, 1978: The expanded north circumpolar vortex of 1976 and winter of 1976–77, and attendant vortex displacement. *Mon. Wea. Rev.*, **106**, 137–142.
- , and —, 1985: Displacements of the north circumpolar vortex during El Niño, 1963–83. *Mon. Wea. Rev.*, **113**, 1627–1630.
- Barnston, A. G., and R. E. Livezey, 1987: Classification, seasonality and persistence of low-frequency atmospheric circulation patterns. *Mon. Wea. Rev.*, **115**, 1083–1126.
- Frauenfeld, O. W., and R. E. Davis, 2000: The influence of El Niño–Southern Oscillation events on the Northern Hemisphere 500 hPa circumpolar vortex. *Geophys. Res. Lett.*, **27**, 537–540.
- , and —, 2002: Midlatitude circulation patterns associated with decadal and interannual Pacific Ocean variability. *Geophys. Res. Lett.*, **29**, 2221, doi:10.1029/2002GL.015743.

- , and —, 2003: Northern Hemisphere circumpolar vortex trends and climate change implications. *J. Geophys. Res.*, **108**, 4423, doi:10.1029/2002JD002958.
- Free, M., and J. K. Angell, 2002: Effect of volcanoes on the vertical temperature profile in radiosonde data. *J. Geophys. Res.*, **107**, 4101, doi:10.1029/2001JD001128.
- Holton, J. R., and H. C. Tan, 1980: The influence of the equatorial quasi-biennial oscillation on the global circulation at 50 mb. *J. Atmos. Sci.*, **37**, 2200–2208.
- Hurrell, J. W., 1996: Influence of variations in the extratropical wintertime teleconnections on Northern Hemisphere temperature. *Geophys. Res. Lett.*, **23**, 665–668.
- Kalnay, E., and Coauthors, 1996: The NCEP–NCAR 40-Year Reanalysis Project. *Bull. Amer. Meteor. Soc.*, **77**, 437–471.
- Kistler, R., and Coauthors, 2001: The NCEP–NCAR 50-year reanalysis: Monthly means CD-ROM and documentation. *Bull. Amer. Meteor. Soc.*, **82**, 247–267.
- Labitzke, K., 1987: Sunspots, the QBO, and the stratospheric temperature in the north polar region. *Geophys. Res. Lett.*, **14**, 535–537.
- , and H. van Loon, 1999: *The Stratosphere: Phenomena, History, and Relevance*. Springer-Verlag, 179 pp.
- , B. Naujokat, and J. K. Angell, 1986: Long-term temperature trends in the middle stratosphere of the Northern Hemisphere. *Adv. Space Res.*, **6**, 7–16.
- Li, J., and J. X. L. Wang, 2003: A modified zonal index and its physical sense. *Geophys. Res. Lett.*, **30**, 1632, doi:10.1029/2003GL017441.
- Miller, A. J., D. R. Cayan, T. P. Barnett, N. E. Graham, and J. M. Oberhuber, 1994: The 1976–77 climate shift of the Pacific Ocean. *Oceanography*, **7**, 21–26.
- Panofsky, H. A., and G. W. Brier, 1958: *Some Applications of Statistics to Meteorology*. The Pennsylvania State University, 224 pp.
- Rosen, R. D., and W. L. Gutowski Jr., 1992: Response of zonal winds and atmospheric angular momentum to a doubling of CO<sub>2</sub>. *J. Climate*, **5**, 1391–1404.
- Thompson, D. W. J., and J. M. Wallace, 1998: The Arctic Oscillation signature in the wintertime geopotential height and temperature fields. *Geophys. Res. Lett.*, **25**, 1297–1300.
- Trenberth, K. E., 1990: Recent observed interdecadal climate changes in the Northern Hemisphere. *Bull. Amer. Meteor. Soc.*, **71**, 988–993.
- , and J. W. Hurrell, 1994: Decadal atmosphere-ocean variations in the Pacific. *Climate Dyn.*, **9**, 303–319.
- van Loon, H., and J. C. Rogers, 1978: The seesaw in winter temperature between Greenland and Northern Europe. Part I: General description. *Mon. Wea. Rev.*, **106**, 296–310.
- , and K. Labitzke, 1988: Association between the 11-year solar cycle, the QBO, and the atmosphere. Part II: Surface and 700 mb in the Northern Hemisphere in winter. *J. Climate*, **1**, 905–920.
- Wallace, J. M., 2000: North Atlantic Oscillation per annular mode: Two paradigms, one phenomenon. *Quart. J. Roy. Meteor. Soc.*, **126**, 791–805.
- Waugh, D. W., 1997: Elliptical diagnostics of stratospheric polar vortices. *Quart. J. Roy. Meteor. Soc.*, **123**, 1725–1748.
- Willett, H. C., 1949: Long-period fluctuations of the general circulation of the atmosphere. *J. Meteor.*, **6**, 34–50.